NANO · MICRO small
www.small-journal.com

High-Performance Li-Ion and Na-Ion Capacitors Based on a Spinel $Li_4Ti_5O_{12}$ Anode and Carbonaceous Cathodes

Manohar Akshay, Shaji Jyothilakshmi, Yun-Sung Lee, and Vanchiappan Aravindan**

Dedicated to Prof. BVR Chowdari on the occasion of his 80th birthday

Lithium-ion hybrid capacitors (LICs) have become promising electrochemical energy storage systems that overcome the limitations of lithium-ion batteries and electrical double-layer capacitors. The asymmetric combination of these devices enhances the overall electrochemical performance by delivering simultaneous energy and power capabilities. Lithium titanate ($Li_4Ti_5O_{12}$, LTO), a spinel zero-strain material, has been studied extensively as an anode material for LIC applications because of its high-rate capability, negligible volume change, and enhanced cycling performance. Here, the different synthetic methods and modifications of the intercalation-type LTO to enhance the overall electrochemical performance of LICs are mainly focused. Moreover, the cathodic part (i.e., the activated carbon derived from various sources, including natural products, polymers, and inorganic materials) is also dealt with as it contributes substantially to the overall performance of the LIC. Not only do the anode and cathode, but also the electrolytes have a substantial influence on LIC performance. The electrolytes used in LTO-based LICs as well as in flexible and bendable configurations are also mentioned. Overall, the previous work along with other available reports on LTO-based LICs in a simplified way is analyzed.

1. Introduction

The 21st century is experiencing dramatic climate change with increased CO, CO_2, NO_2, and other harmful gas emissions. The main contributors to climate change are the fossil fuels that are burned by vehicles, industries, and power stations. In addition to their environmental impacts, the consumption of fossil fuels can also exhaust energy resources for future generations. Hence, electrochemical energy storage devices have been proposed as replacements for fossil fuels. Electrochemical energy storage devices include batteries, supercapacitors, and fuel cells. Batteries are energy storage devices that convert the energy stored in the active material to electrical energy by electrochemical reactions. Earlier rechargeable batteries were based on lead–acid, Ni–Cd, and metal hydrides. After their introduction, lithium-ion batteries (LIBs) became predominant in the electronic market. LIBs are widespread energy storage devices with a high energy density and low self-discharge, which has resulted in their increased demand for use in electric vehicles (EVs) and aerospace applications.[1–3] However, the main challenges LIBs face are their power capabilities and long cycle life. A supercapacitor is another electrochemical energy storage device that replaces batteries in certain applications because it has a high-power density and long cycle life (>1,00,000 cycles) compared to rechargeable batteries.

Studies on a single system with both high energy density and high power density have resulted in the development of a new class of supercapacitors: hybrid supercapacitors (HSC).[4,5] The term "hybrid" indicates the energy storage mechanism. These devices have electrodes with both faradaic and non-faradaic energy storage mechanisms. The anode stores energy electrochemically, whereas the cathode stores energy electrostatically. One end of the HSC is the battery-type electrode ($Li_4Ti_5O_{12,}$ lithium titanium oxide, LTO), graphite, or transition metal oxides), and the other end is the electrical double-layer capacitor (EDLC) electrode. The combination of two different electrodes enhances the electrochemical performance thanks to the synergic effect. Among hybrid storage devices, lithium-ion capacitors (LICs) have received increased attention because of their simultaneous high power and high energy density in a single device.[6–8] LICs exhibit higher power density than batteries and higher energy density than supercapacitors. However, compared with batteries and fuel cells, LICs are still inferior in terms of energy density. Moreover, their power density must be enhanced to compete with EDLCs.[9] The electrodes in LICs play a vital role in determining their performance in terms of energy and power density. The electrodes that have been tested for LICs include pre-lithiated graphitic carbon and LTO. The former is already on the market, and such a configuration is

M. Akshay, S. Jyothilakshmi, V. Aravindan
Department of Chemistry
Indian Institute of Science Education and Research (IISER)
Tirupati, Andhra Pradesh 517507, India
E-mail: aravindan@iisertirupati.ac.in
Y.-S. Lee
School of Chemical Engineering
Chonnam National University
Gwangju 61186, Republic of Korea
E-mail: leeys@chonnam.ac.kr
The ORCID identification number(s) for the author(s) of this article can be found under https://doi.org/10.1002/smll.202307248

DOI: 10.1002/smll.202307248

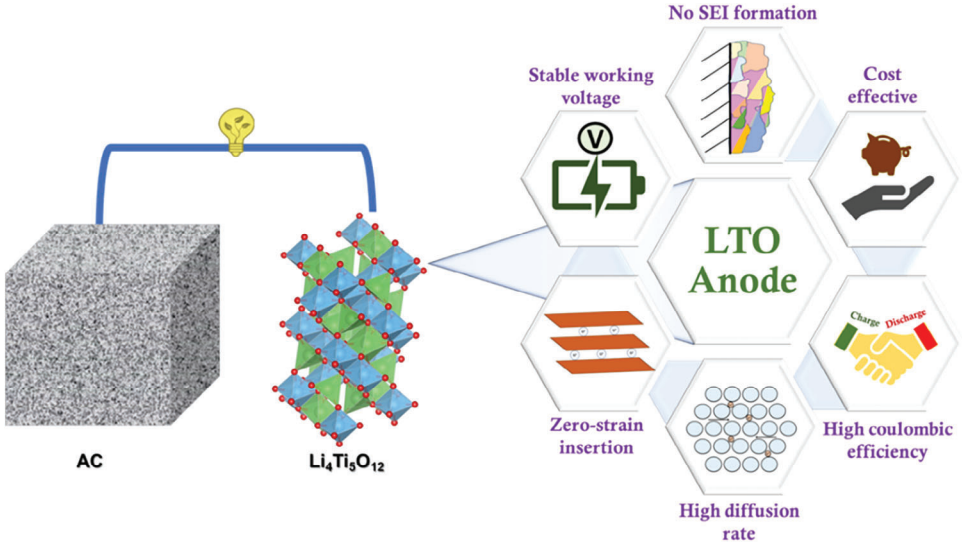

Figure 1. Schematic representation of the typical LIC based on LTO anode and its benefits.

considered an energy variant of the LIC, owing to the wide electrochemical activity. On the other hand, the LICs based on LTO are treated as a powered variant of the LIC assembly. However, both variants employ high-surface-area activated carbon (AC) as a capacitive component in aprotic organic solutions.[10,11] Hence, various anode and cathode materials have been explored, and some have reached the commercialization stage, among which LTO is notable.

2. LTO Anode

LTO has long been investigated and is considered a promising anode material for LIBs. LTO has been commercialized with spinel cathodes (e.g., $LiMn_2O_4$ and its derivatives). The spinel structure and morphology of LTO, along with its outstanding properties, including a stable operating voltage (1.55 V vs Li) and high Coulombic efficiency (≈100%), negligible volume change during the charge-discharge process, zero-strain insertion, no solid electrolyte interface (SEI) formation, low cost, and safety play a crucial role in the electrochemical performance of these cathodes (**Figure 1**). LTO is a good alternative for carbon-based anodes like graphite because it agrees with their theoretical (175 mAh g^{-1}) and practical specific capacity (>170 mAh g^{-1}). The mechanism involved in the intercalation of Li-ions into LTO can be represented as $Li_4Ti_5O_{12} + 3Li^+ + 3e^- = Li_7Ti_5O_{12}$. This reaction can be written as spinel $[Li]_{8a}[Li_{1/3}Ti_{5/3}]_{16d}O_4$ to the rock-salt structure $[Li_2]_{16c}[Li_{1/3}Ti_{5/3}]_{16d}O_4$.

As LTO enables fast charging and provides a high current, it is expected to become the power source of EVs in the future. LTO as a negative electrode in the LIC (AC/LTO) system in the presence of aprotic organic electrolytes was first proposed by Amatucci et al.[12] In contrast to LIBs, LTO-based LICs have undergone tremendous development and have been recently commercialized by Pureechem. The AC/LTO exhibits an energy density of >80% and a specific capacitance of >20% compared to the conventional EDLC. Thus, LTO delivers adequate electrochemical performance in LICs, although they still struggle to meet certain standards required for HEVs and EVs. In this context, research attention is being focused on the development of a high-performance battery component by incorporating various techniques and methodologies.

The poor Li^+ diffusion and electronic conductivity of pristine LTO are drawbacks that researchers have tried to mitigate to enhance electrochemical performance, using approaches like nanosizing, element-doping, carbon coating, and hybridization with carbon and metal powders. Pre-lithiation is considered an excellent method to nullify the sudden cell voltage drop/rise during the charge/discharge process in the LTO anode and compensate for the energy loss during the initial cycle that is due to the high initial potential of the AC cathode in LICs.[13] Divya et al.[14] studied the role of the pre-lithiation of LTO in LICs by varying the pre-lithiation levels ($Li_{4+x}Ti_5O_{12}$, $0 \le x \le 3$). They concluded that the pre-lithiation step is not crucial for the assembly of LICs. However, an optimal pre-treatment guarantees the cycling stability of LICs by providing a lithium inventory. **Figure 2**a shows a comparison of CV profiles of LICs fabricated with different pre-lithiation levels at a scan rate of 1 mV s^{-1} and illustrates the complete voltage window utilization in the case of the AC/$Li_5Ti_5O_{12}$ assembly compared with $Li_4Ti_5O_{12}$ and $Li_7Ti_5O_{12}$ LICs. The long-term stability performance of the assembled LICs at a current density of 1 A g^{-1} is shown in Figure 2d. The AC/$Li_7Ti_5O_{12}$ cells worked for more than 1000 cycles without any noticeable decrease in capacity compared to other cells (one with partial and the other without pre-lithiation). The capacity fading in other LICs may be due to the loss of lithium inventory or the loss of active material in the lithiated/de-lithiated state. In 2007, JM Energy Corporation (now Musashi Energy Solutions) commercialized the first prismatic "Ultimo LIC" using pre-lithiated graphite coupled with AC patented by Fuji Heavy Industry.[10,15] The electrode mass ratio and volume ratio are the main components of the specific capacity and energy density, respectively. The optimal pre-lithiation capacity range is closely related to the cathode and anode mass ratio and the initial potential of the AC cathode. As the electrode mass ratio increases, the minimum pre-lithiation

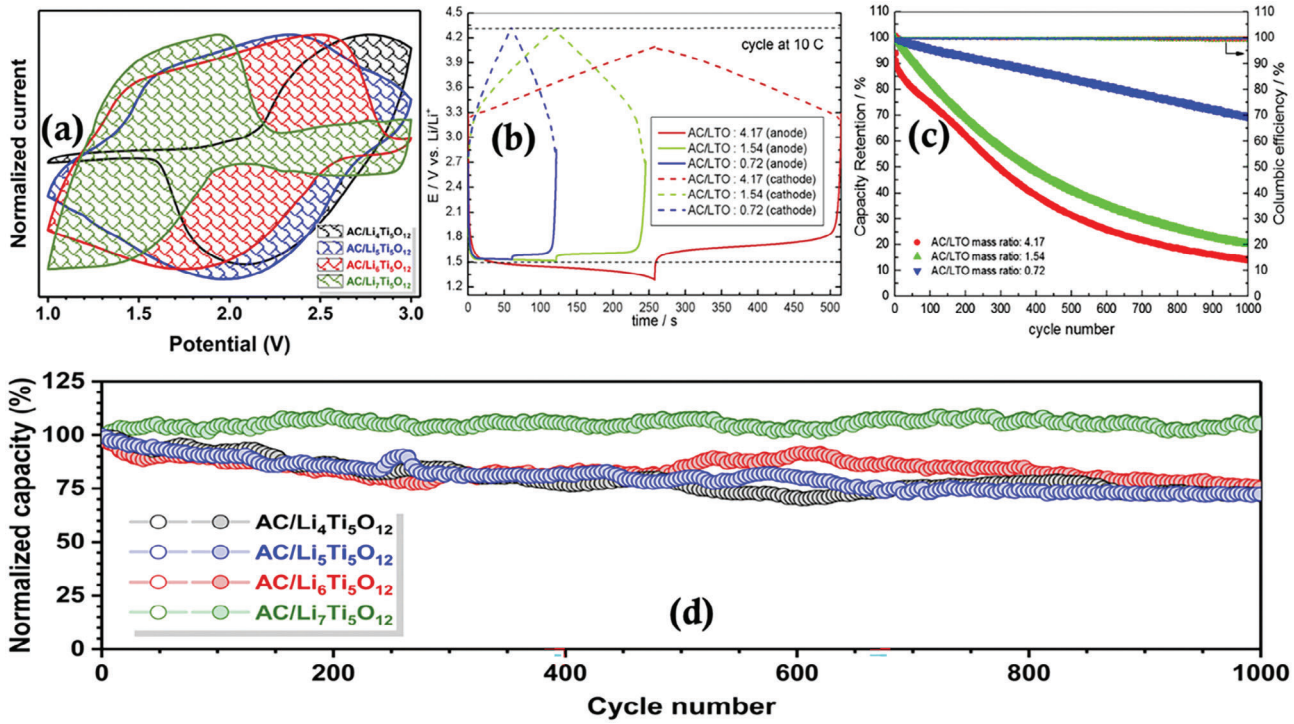

Figure 2. (a) Comparison of CV profiles of all four LICs at a scan rate of 1 mV s^{-1}. Reprinted with permission.[14] Copyright 2022, Royal Society of Chemistry, (b) anode and cathode voltage profiles of asymmetric cells with AC/LTO mass ratios of 4.17, 1.54, and 0.72 at a 10 C rate, (c) capacity retention at 10 C over 1000 cycles for the three asymmetric systems. Reprinted with permission.[16] Copyright 2015, Elsevier, and (d) long-term cycling performance of the assembled LICs at a current density of 1 A g^{-1}.Reprinted with permission.[14] Copyright 2022, Royal Society of Chemistry. The black dotted lines represent the ideal voltage limit for the cathode and anode.

capacity gradually increases. Dsoke et al.[16] suggested the importance of the modulation of the electrode mass ratio in LICs. Through AC/LTO mass optimization, various hybrid systems with different rate capabilities can be fabricated for practical applications. These authors lowered the electrode mass ratio from 4.17 to 1.54 and then to 0.72. The device with the cathode/anode mass ratio of 0.72 delivered an energy density of 31 Wh L^{-1}. Further, the authors demonstrated that lowering the AC/LTO mass ratio leads to a lower AC thickness and, consequently, to a lower diffusion resistance, which improves the cycling stability, results in less pronounced anode polarization, and minimizes the decomposition of the electrolyte on the anode surface. Figure 2b displays the anode and cathode voltage profiles of asymmetric cells with AC/LTO mass ratios of 4.17, 1.54, and 0.72 at a 10 C rate. Figure 2c shows that the cell balanced with the lowest AC/LTO mass ratio is more stable than the other two cells. Lee et al.[17] reported that carbon coating on the LTO anode is another promising method to improve the conductivity and the Li-ion diffusion, resulting in high rate capability and cycling stability. It was observed that, with an increasing carbonization time, the thickness and uniformity of the carbon layer increase, resulting in a lowered capacity because of the decreased region of Li-ion intercalation/deintercalation and the existence of an intermediate thick carbon phase. Lv et al.[18] reported the synthesis of LTO electrodes via a solvent-free method based on electrostatic spraying deposition technology, which improved the porous nature of the microstructured electrodes with a large electrochemically active surface area. A microporous electrode enhances electrolyte infiltration and Li-ion diffusion, leading to faster Li-ion transportation and enhanced rate performance compared to conventional wet-coated electrodes. The dry-sprayed LTO electrodes delivered a high reversible capacity of 117 mAh g^{-1}, which was much higher than that of wet-coated LTO electrodes (91 mAh g^{-1}) at a 10 C rate. Recently, Bhowmik et al.[19] fabricated a hybrid LIC with LTO as an anode coupled with a composite cathode of LNMO and a high-surface-area carbon (HSAC). Different ratios were tested to optimize the composition of LNMO and HSAC according to the percentage of HSAC (50, 60, 70, and 80%). The LIC assembled with 80% HSAC and LNMO as a cathode and pre-lithiated carbon-coated LTO exhibited higher capacity and cycling stability with a maximum energy density of 48 Wh kg^{-1} at a power density of 250 W kg^{-1}.

2.1. Effects of Using Additives

In some reports, certain additives like graphene[11,20–25] and carbon nano-fibers[11,26,27] rather than commercial ones have been added to LTO to enhance electrochemical performance. Carbonaceous additives like graphene increase the electrical conductivity, surface area, and pore volume, which improve contact with the electrolyte, shorten the Li^+ diffusion length, and facilitate electron and ion transport during the lithiation/de-lithiation process. A graphene-inserted LTO composite anode (G–LTO) and a three-dimensional porous graphene-sucrose cathode were fabricated by Leng et al.[23] for an advanced graphene-based hybrid

system. The optimized hybrid system displayed an ultrahigh energy density of 95 Wh kg^{-1} at a 0.4 C current rate. Similarly, Xu et al.[24] synthesized LTO-graphene using a two-step method to attain an AC/LTO-graphene configuration, which delivered a high energy density of 22 Wh kg^{-1} after 10 000 cycles. Zhang et al.[25] reported that LTO with a fine and porous microstructure can be obtained by low-temperature sintering (600 °C) and delivers a specific capacity of 65 mAh g^{-1} at a 20 C current rate. As the temperature increases, the LTO particles tend to grow into coarse particles and agglomerates, deteriorating the electrochemical performance (14 mAh g^{-1} at a 20 C rate). After a hydrothermal/solvothermal reaction, the sintering treatment substantially affects the crystallinity, defect density, microstructure, and electrochemical properties. The LIC fabricated using this G-LTO after sintering as the anode and AC as the cathode delivered a maximum energy of 44 Wh kg^{-1} with excellent cycling stability (a capacity retention of 80% after 10,000 cycles). An improved reversible capacity of 121 mAh g^{-1} at an extremely high current rate of 100 C was achieved by Wang et al.[28] The excellent cyclic stability (90% capacity retention at 20 C) with ≈100% Coulombic efficiency after 2500 cycles is worth mentioning.

2.2. Modifications of the Synthetic Methods

Various LTO synthetic routes have been adopted to enhance scalability, crystallinity, and purity.[29] The particle size reduction of the active material to the nanoscale promotes shorter solid-state diffusion pathways for Li-ions, resulting in a rapid increase in electrode kinetics and higher rate capability. Raj et al.[30] synthesized spinel LTO employing a solid-state route by ball milling at 900 rpm for 12 h to mix TiO_2 and Li_2CO_3; the mixture was dried at 100 °C, followed by calcination at 800 °C for 10 h. These authors compared the electrochemical characteristics of AC-based EDLCs and LICs. The LIC showed discharge capacities of 13 and 10 mAh g^{-1} at current rates of 0.5 and 1 C, respectively, with capacity retention of >86%, which were higher values than those displayed by the EDLCs (9 and 3 mAh g^{-1}, respectively, along with 80% capacity retention). Cheng et al.[31] synthesized nano-sized LTO particles using the molten salt process with LiCl as a high-temperature flux that showed a discharge capacity of 159 mAh g^{-1} and capacity retention as high as 60%, even at a high rate of 100 C. It is important to note that the electric conductivity of the nanomaterial should be improved to boost the power performance.

To enhance the Li^+ ion diffusion coefficient and electrical conductivity, Naoi et al.[27] prepared nano-crystalline LTO (*nc*-LTO) nested and grafted onto carbon nanofibers by a simple mechanochemical sol-gel reaction under ultra-centrifugal (UC) force, followed by heat treatment. *nc*-LTO@CNF/AC-based LIC achieved a high energy density and power density of 40 Wh L^{-1} and 7.5 kW L^{-1} per electrode volume, respectively. Furthermore, these authors replaced CNF with a supergrowth carbon nanotube[32] (SGCNT) as the matrix for the LTO because of its high elemental purity, high electrical conductivity, and high specific area. The half-cell Li/UC-LTO@SGCNT exhibited high capacities of 130 and 107 mAh g^{-1} at 10 and 300 C rates, respectively, with a capacity retention of 60% even at a 1200 C rate. The nanohybrid capacitor fabricated with this UC-LTO@SGCNT showed 4.5 times higher energy density than the conventional EDLC.[26] Even though the solid-state and sol–gel reaction processes are suitable for large-scale fabrication, they cannot be used to synthesize LTO with particle sizes <300 nm, as the particle size may strongly affect their high-rate performance during the charge–discharge process. Therefore, modern high-energy mechanical milling is employed to facilitate pulverization to obtain a powder with nanoscale particle size by mechanical force that produces materials with metastable and nano-crystalline phases. Lee et al.[33] fabricated LTO by high-energy mechanical milling at 3500 rpm and post-calcination to improve the crystallinity of the powder. When mechanical milling is used for pulverization, the powder particles either remain unchanged or are fractured into smaller particles. These authors observed that post-calcination at a moderate temperature is more effective for improving the crystallinity of pulverized LTO as well as the electrochemical performance. A 100-nm-sized LTO was fabricated by optimizing the high-energy milling and post-calcination at 700 °C. The 100-nm-sized LTO exhibited high-rate capability and capacity retention of 99.9% even after 1500 cycles. Notably, improved crystallinity and particle size reduction by post-calcination and mechanical milling results in excellent rate capability. Co-polymerization and a post-CO_2 activation process were employed to attain nanosized LTO crystals uniformly embedded on a mesoporous-AC matrix, forming a highly conductive composite material as reported by Jiang et al.[34] As the mesoporous-AC content increased, the electronic conductivity and Li-ion transfer at the electrode/electrolyte interface were improved along with an elevated rate capability and cycling stability for LTO-AC hybrid anodes. LTO-AC/AC-based LIC with an AC content of 54 wt% displayed a high energy density of 38 Wh kg^{-1} with a capacity retention of 67% and energy density retention of 90.8% after 2000 cycles at a current rate of 1 A g^{-1}.

Even though numerous methods have been adopted to improve the performance of LTO-based LICs, it is challenging to reach the energy goal needed for commercialization. Thus, to address large-scale application demands (e.g., trolleybuses), Ruan et al.[35] prepared a 700-F hybrid capacitor pouch cell comprising ≈240-mm-thick AC cathodes and ≈60-mm-thick LTO anodes in a 1.2 M solution of $LiPF_6$ in a propylene carbonate/ethylene carbonate/ethyl methyl carbonate (PC/EC/EMC) mixture as an electrolyte. The micro spherical LTO was synthesized by spray-drying where anatase TiO_2, Li_2CO_3, and diethylene glycol were ball-milled in the presence of deionized water and then spray-dried, followed by calcination at 800 °C for 10 h under an air atmosphere. The 700-F hybrid capacitor showed maximum energy and power density of 51.65 Wh kg^{-1} and 2.466 kW kg^{-1}, respectively, with an ultra-long cycle lifetime (≈92% capacity retention after 10 000 cycles) and high-rate capability.

3. Cathode

This review also discusses the different carbon cathode materials used with LTO anode-based Li- and Na-ion capacitors (LICs and NICs). The cathode material used in LIC and NIC mainly comprises different forms of carbon derived from various sources (natural products, polymers, or inorganic materials). The cathode also plays a vital role in determining the performance of LICs and NICs. However, research has focused primarily on the

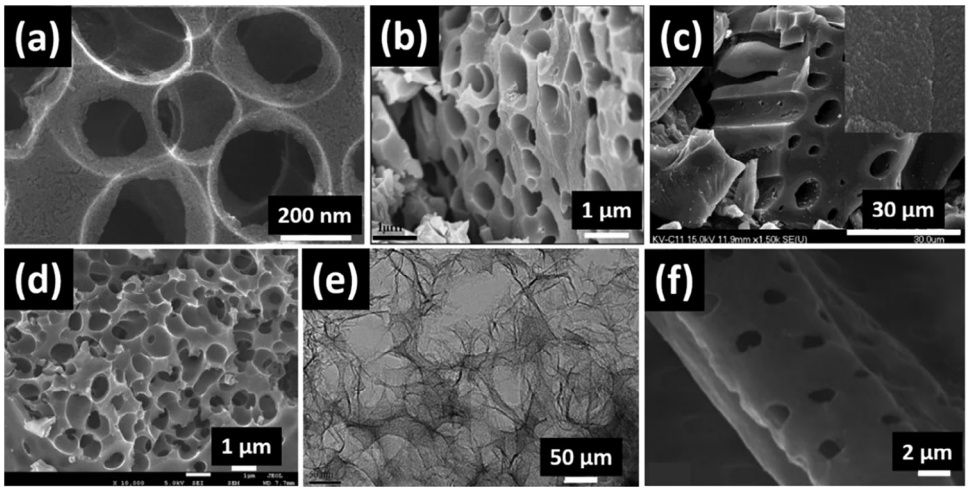

Figure 3. SEM/TEM images of carbon derived from various natural products: (a) waste paper. Reprinted with permission.[37] Copyright 2014, John Wiley and Sons, (b) human hair. Reprinted with permission.[39] Copyright 2015, Elsevier, (c) Prosopis juliflora. Reprinted with permission.[40] Copyright 2015, Elsevier, (d) orange peel. Reprinted with permission.[43] Copyright 2017, John Wiley and Sons, (e) rubberwood. Reprinted with permission.[45] Copyright 2020, Elsevier, and (f) sugarcane bagasse. Reprinted with ref. [46] Copyright 2021, The Authors under a Creative Commons Attribution 3.0 International License, Published by Institute of Physics.

anode as it determines the overall energy density of the hybrid capacitors, although the high-surface-area AC has a crucial role in determining the power density. The charge storage in the cathode is achieved via a reversible, non-Faradaic adsorption/desorption reaction of anions on the surface of the AC. The fast diffusion of anions between the electrode and electrolyte provides an enhanced power density for the HCs. Hence, numerous attempts have been made to derive AC from various sources. Several research groups have tested the synthesized AC as the cathode for LIC, for which they have used the commercially available LTO anode.

3.1. Natural Products

Natural products consist of hydrocarbon, which is heated at high temperatures to yield carbonaceous materials. Two major processes are involved in the conversion of the raw material into a carbonaceous material: i) high-temperature calcination and ii) activation using certain reagents (NaOH or KOH). Many researchers have optimized the heating temperature, dwelling time, and other factors to generate high-surface-area carbon. Activating the resulting carbon using various agents can increase the surface area and porosity to a great extent. Hence, various studies have been published (and many are in progress) to obtain high-surface-area AC for use as the cathode for LIC. Jain et al.[36] reported the synthesis of a carbonaceous material using coconut shells as the precursor. The resulting AC exhibited ≈60% mesoporosity with a surface area of 1652 $m^2\ g^{-1}$. The LIC fabricated using the obtained carbon as the cathode delivered a maximum energy density of 69 Wh kg^{-1}. The cyclic performance of the LIC attained 85% capacity retention even after 2000 charge-discharge cycles. Puthusseri et al.[37] converted shredded waste paper (office waste) into porous AC, using a straightforward two-step procedure comprising a hydrothermal treatment and high-temperature pyrolysis. As a result, three-dimensionally connected hierarchical porous carbon with a high surface area was obtained. The SEM images in **Figure 3**a reveal the different-sized (micro, meso, and macro) interconnected porous morphology. The BET surface area was ≈2341 $m^2\ g^{-1}$, which was higher than that previously reported for AC derived from waste newspaper (≈416 $m^2\ g^{-1}$).[38] These authors fabricated both supercapacitors and LIC with this porous AC and used a gel electrolyte to replace the conventional liquid-based electrolyte. The performance of their fabricated supercapacitor was fascinating. They obtained a maximum energy density of 58 Wh kg^{-1} for their supercapacitor, and their LIC had a maximum energy density of 62 Wh kg^{-1}.

An interesting carbon source as the cathode for LIC was reported by Satish et al.[39] This author used a cheap and easily available carbon source (human hair) as the precursor for the AC synthesis. The pre-treatment, followed by activation with NaOH, resulted in a high-surface-area AC (1116 $m^2\ g^{-1}$). The explosive activation resulted in large pores over the flaky-natured structure observed in the SEM images (Figure 3b). The fabricated AC/LTO assembly had an energy density of 22.5 Wh kg^{-1}. Sennu et al.[40] reported the use of the undesirable *Prosopis juliflora* plant to produce AC. *P. juliflora* is an invasive plant that contributes to mosquito proliferation and malaria transmission but can be efficiently transformed into useful carbon for the cathode of LIC. A cracked and flaked type morphology was obtained after the activation of the carbon with KOH as a result of gasification at high temperatures (Figure 3c). The fabricated LIC delivered an energy density of 80 Wh kg^{-1} with 76% capacity retention when used for more than 10 000 cycles. Rice husk[41] was also used as a precursor for the synthesis of high-surface-area AC. The carbon was activated using two agents (KOH and H_3PO_4), with the carbon activated with KOH showing higher electrochemical performance. The obtained high-surface-area AC (2303 $m^2\ g^{-1}$) and LTO-based LIC yielded a maximum energy density of 57 Wh kg^{-1}.

Teak sawdust from the timber industry was used to produce carbon for the cathode by Jain and co-workers.[42] They adopted

three strategies. A high-surface-area mesopore AC was synthesized either by i) an H_2O_2-mediated hydrothermal pre-treatment, ii) without H_2O_2 pre-treatment, and iii) an H_2O_2-mediated pre-treatment with the addition of benzene tetracarboxylic acid (BTA) as a processing agent. The largest mesopore area and BET surface area (2108 m^2 g^{-1}) were obtained with (iii). Moreover, the LIC with an LTO anode and teak-wood-derived AC cathode exhibited moderate energy and power capabilities. The fabricated LIC delivered a maximum energy density of 53 Wh kg^{-1}. Maharjan et al.[43] developed a high-surface-area AC using orange peel (OP), another interesting use of biowaste for this purpose. The interconnected porous structure (Figure 3d) enhanced the specific capacitance by providing more active sites for the formation of the double layer. These researchers analyzed different capacitor configurations, such as OP-AC/OP-AC (organic and aqueous), OP-AC/LTO, and OP-AC/LiC_6. Among these, the OP-AC/LTO-based LIC exhibited an energy density of ≈35 Wh kg^{-1} with a capacity retention of ≈82.2% after 2500 cycles. AC was also prepared by carbonization and activation of corncob [44] using KOH as the activating agent at 850 °C for 3 h, followed by ball milling. The corncob-based LIC achieved a maximum energy density of 79.6 Wh kg^{-1} and an excellent capacity retention of 85.2% after 2000 cycles. The optimized corncob-based LIC exhibited higher performance than commercial AC, and the power density was twice that of rechargeable LIBs. Lin et al.[45] pyrolyzed rubberwood to obtain the AC and tested its performance in a symmetric capacitor and LIC. The obtained carbon exhibited a spherical nanoporous structure based on the SEM images (Figure 3e). The fabricated symmetric supercapacitor delivered a specific capacitance of 136 F g^{-1} at a current of 0.5 mA in 1 M $LiClO_4$/PC and stability for 40,000 consecutive cycles. The LIC with a modified LTO anode and rubberwood-derived carbon displayed a maximum energy density of 142 Wh kg^{-1}. Moreover, 85.7% capacity retention was reported, even after 10 000 cycles. Sugarcane bagasse[46] was used to produce AC (SBAC) as a cathode material in LIC. The carbon pyrolyzed at 840 °C exhibited a honeycomb-like morphology with many pores (Figure 3f). The assembled SBAC/LTO-based LIC produced a maximum specific energy of 35.49 Wh kg^{-1} and a high specific power of 2.95 kW kg^{-1}.

3.2. Polymer-Based Carbons

Porous carbons have been evaluated as cathodes for LIC as they have a high surface area. The synthesis of AC from natural sources involves an initial heat treatment followed by activation. This method is useful for the structural modification of carbon to micro and mesoporous levels. However, tuning the AC to the desired morphology with the required properties is very difficult with this synthetic route. Hence, polymers are used as precursors.

Puthusseri et al.[47] obtained high-surface-area porous carbon (HSPC) from a poly(acrylamide-co-acrylic acid) potassium salt without any activating agent. The obtained HSPC had a specific surface area of 1490 m^2 g^{-1} and delivered a maximum energy density of ≈55 Wh kg^{-1} in the LIC assembly. Moreover, the capacity retention was also high, with ≈87% of the initial value after 2000 cycles. Gokhale et al.[48] transformed the 4-amino benzoic acid monomer into an oligomer salt using a facile free radical polymerization process. The oligomer salt was pyrolyzed to obtain high-surface-area carbon. The LIC fabricated using this carbon exhibited a maximum energy density of 63 Wh kg^{-1}. Similarly, Chhatre et al.[49] derived polystyrene using click chemistry and obtained a high-surface-area (1860 m^2 g^{-1}) carbon. The LIC with this graphene-like framework with high porosity displayed an energy density of 61 Wh kg^{-1} with 70% capacity retention even after 2000 cycles.

AC can be prepared from a wide variety of natural products. Among them, corncob-derived AC exhibited the largest surface area. However, considering the electrochemical performance of LIC with an LTO anode, the rubberwood-derived AC exhibited the highest energy density, whereas the waste paper-derived AC achieved the highest power density. For an easy comparison, we summarized the performance of the LICs in **Table 1**.

3.3. Graphene-Based Carbons

Apart from natural products and polymers, the cathode materials for LICs can also be obtained from different forms of graphene. Several studies have been reported on the use of different forms of graphene as the electrode for supercapacitors, as graphene is a prospective material for electrochemical energy storage. Aravindan et al.[51] used trigol-reduced graphene oxide (TRGO) as the positive electrode for LIC. The obtained LIC exhibited a promising performance, with a maximum energy density of 45 Wh kg^{-1} and cyclic stability for ≈5000 cycles. Another type of material is the metal-organic framework (MOF), which was first reported by Banerjee et al.[52] These researchers used Zn-based MOF as the precursor to obtain high-surface-area porous carbon. The MOF-DC/LTO-based LIC delivered an energy density of 65 Wh kg^{-1} with long-term cyclic stability for 10,000 cycles and 82% capacity retention. Porous graphene was also used as the cathode material for the hybrid capacitor.[53] The LIC, using a 3D porous graphene macroform (PGM) as the positive electrode, delivered a maximum energy density of 72 Wh kg^{-1}. In addition, it exhibited cyclic stability for 1000 cycles with 65% capacity retention. Mhamane et al.[54] synthesized reduced graphene oxide (rGO) by a bottom-up approach where the sp^2 carbon-rich 1,2,4,5-benzene tetracarboxylic acid (BTCA) was used as the precursor. The BTCA-derived carbon (BTCADC) exhibited a 960 m^2 g^{-1} surface area, which was almost two-fold higher than that of the rGO. Moreover, the surface area was increased to 2673 m^2 g^{-1} via a chemical activation process (using KOH) to form activated BTCADC (A-BTCADC). The LIC fabricated with both BTCADC and A-BTCADC delivered a maximum energy density of ≈43 and 63 Wh kg^{-1}, respectively, which is better than that of a commercially available AC with an LTO anode (≈36.08 Wh kg^{-1}). The LIC also exhibited high cyclic stability for 6000 cycles with a capacity retention of 97%. Porous graphene belts were synthesized by Ma et al.[55] using the chemical vapor deposition method. The LIC prepared with this cathode delivered an energy density of 120 Wh kg^{-1}. The abundant pore channels and the robust belt-like structure enhanced the capacitive performance. Suryawanshi et al.[56] conducted a comparative study of the electrochemical performance of four ACs synthesized using different methods. The four dif-

Table 1. Comparison of the physical and electrochemical parameters of the different types of carbon.

-/LTO	Surface area [m^2 g^{-1}]	Energy density [Wh kg^{-1}]	Power density [kW kg^{-1}]	Cycling stability [cycles]	Capacity retention [%]	Refs.
Biomass						
Coconut shell	1652	69	–	2000	85	[36]
Waste paper	2341	62	13	5000	85	[37]
Human hair	1116	23	2	1000	80	[39]
Prosopis juliflora	2410	80	3	10,000	76	[40]
Rice husk	2303	57	4.3	2000	92	[41]
Teak sawdust	2108	53	–	2000	–	[42]
Orange peel	1901	35	–	2500	82.2	[43]
Corncob	2646	79.6	4	2000	85.2	[44]
Rubberwood	1365	142	4.556	10,000	85.7	[45]
Sugarcane bagasse	2236.9	35.49	2.95	–	–	[46]
Polymers						
Porous carbon	1490	55	–	2000	87	[47]
Oligomer salt	1381	63	10	1000	81	[48]
Polystyrene	1860	61	10.015	2000	70	[49]
Polypyrrole	3268	87	0.198	3000	90.2	[50]
Graphene						
Trigol-reduced graphene oxide	56	45	3.3	5000	–	[51]
MOF-derived 3D carbon cubes	2714	65	–	10,000	82	[52]
3D porous graphene macroform	373	73	0.65	1000	65	[53]
Macro-graphene sheet-like carbon	2673	63	0.5	6000	97	[54]
Porous graphene belt	978	120	8.044	2000	83.7	[55]
Perforated graphene	260	65	0.5	1000	99.5	[56]

ferent sources were hierarchically perforated graphene (HPGN), a polymer (poly (4-styrene sulfonic acid-co-maleic acid) sodium salt)-derived graphene, dead neem leaf-derived carbon, and commercial activated carbon. Among these LICs, HPGN/LTO exhibited the best performance because of its appropriate porosity and high-conductance graphitized structure. HPGN/LTO delivered a maximum energy density of 65 Wh kg^{-1} and long-term cyclic stability with a capacitive retention of 99.5% even after 1000 cycles. Another AC was derived from polypyrrole[50] and exhibited an even higher energy density (87 Wh kg^{-1}).

3.4. Importance of Tuning the Electrolyte

We have described the performance of LIC with LTO and AC derived from different methods/materials. In the case of the negative electrode, different precursors were used to obtain a high-performance anode. On the other hand, the AC was derived from various sources, including natural products, polymers, and graphene. Moreover, different activation procedures were employed to enhance the surface area and, thereby, the performance of the anode. Not only do the anode and cathode contribute to the performance of the LIC, but the electrolyte as well. The electrolyte has a leading role in the enhancement of the overall performance of the LIC. Nonetheless, there are few studies focused on the electrolyte where the commercial LTO anode and AC cathode have been used.

One such study used lithium salt in PC as the electrolyte for the LIC.[57] The primary issue with the PC is its decomposition beyond 3 V vs Li, leading to swelling of the LTO anode through gassing, thereby affecting the electrochemical performance. This issue was tackled using supporting electrolytes. Chikaoka et al.[58] applied a dual-ion concept where they incorporated an additional salt (spiro(1,1′)-bipyrrolidinium tetrafluoroborate, $SBPBF_4$) into the lithium-based electrolyte (1 M lithium tetrafluoroborate, $LiBF_4$ in PC). This reduced gassing by 35–50% and enhanced ionic conductivity, which translated to enhanced performance for the LIC. Iwama et al.[59] replaced the PC with a hydrolysis-resistant solvent (ethyl isopropyl sulfone, EiPS), which helped in the high-potential (3.3 V vs Li) operation of LTO without any degradation.

Chikaoka et al.[58] also studied the improvement in electronic conductivity by coating the LTO with increased thickness. They fabricated an electrode with a thickness of a few hundred μm and evaluated its conductivity. The dual-cation electrolyte exhibited increased conductivity, and decreased ohmic drops were observed. The critical parameter is the availability of ions during the insertion into the LTO. In the case of a single-cation electrolyte, only the solvated Li^+ ions are available for conduction. By contrast, in a dual-cation electrolyte, both ions (solvated Li^+ and SBP^+) participate in the conduction, thereby increasing the overall conductivity. After the dual-cation concept was popularized, different cations were introduced, and their performance was analyzed. Various electrolytes having dual cations employing $LiBF_4$ with $SBPBF_4$, $EMIBF_4$, $TEMABF_4$, and

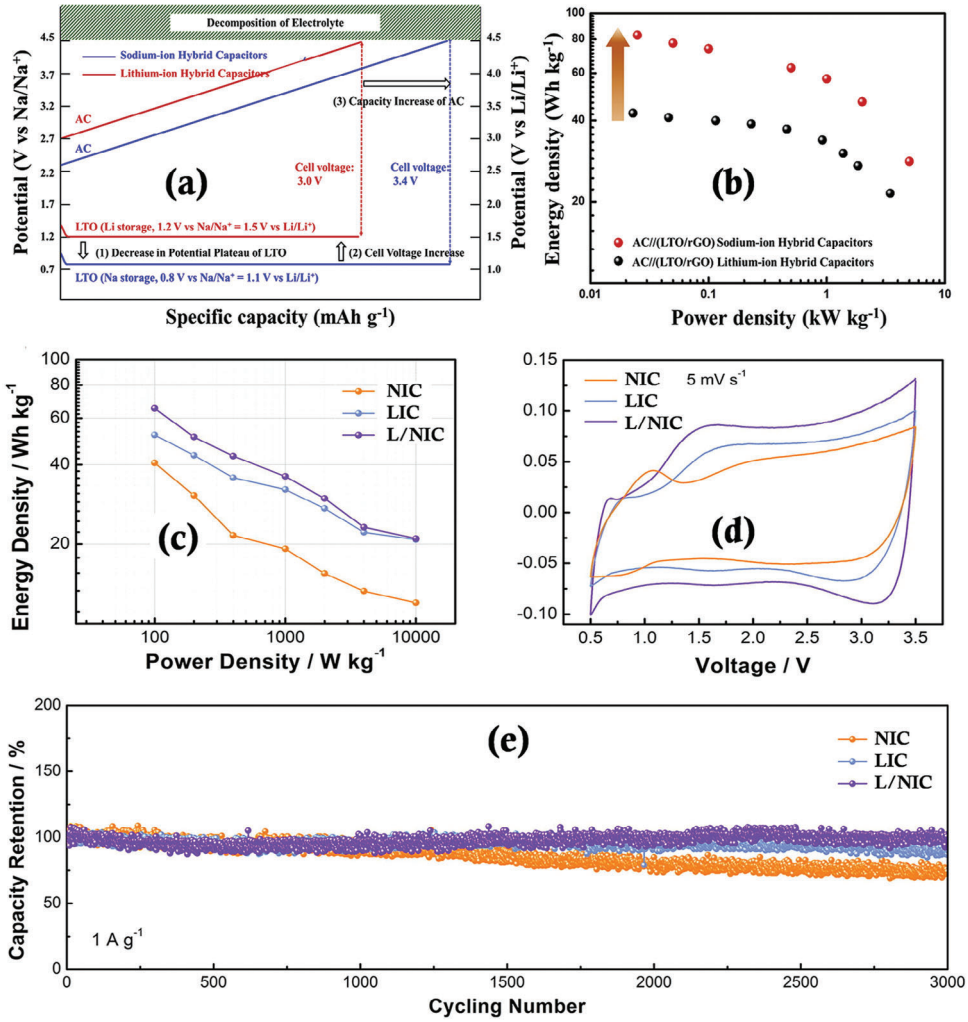

Figure 4. (a) Voltage profiles of the LTO anode and AC cathode in the AC/LTO NICs and AC/LTO LICs, (b) comparison of the energy densities and power densities of the NICs and LICs. Reprinted with permission.[20] Copyright 2018, Elsevier, (c) CV curves of all as-constructed hybrid capacitors at a scan rate of 5 mV s^{-1}, (d) Ragone plots for NIC, LIC, and L/NIC, and (e) a comparison of cycling stability over 3000 cycles for three configurations. Reprinted with permission.[65] Copyright 2021, Elsevier.

$TEABF_4$ have also been designed to enhance the overall ionic conductivity and electrochemical performance of LICs.[57,58,60] One such electrolyte was $LiBF_4$ with $SBPBF_4$ in the low-viscosity, low-dielectric-constant solvent dimethyl carbonate (DMC). This dual-ion electrolyte exhibited a tenfold increase in conductivity (5.7 mS cm^{-1}) compared to the single-cation electrolyte (1 M $LiBF_4$/DMC, 0.5 mS cm^{-1}).[61] Some studies have reported changes in the LTO properties when contact with electrolytes,[62] and others have compared electrolytes to investigate the gas-swelling behavior.[63]

4. LTO as an Anode in NIC

The Na-insertion/extraction process into/from LTO has recently gained considerable attention as a possible alternative for lithium, owing to sodium's abundance and low cost. Unlike the straightforward Li-insertion ($Li_7Ti_5O_{12}$), LTO undergoes a three-phase Na-storage process, in which LTO forms two new phases in the following manner: i) the formation of the Na_6Li phase through the occupation of Na^+ in the 16*c* sites, ii) and the migration of Li_{8a} into the nearest Li_4 sites leads to the formation of the Li_7 ($Li_7Ti_5O_{12}$) phase.[64] Therefore, overall, the three-phase Na-storage mechanism can be written as

$$2Li_4Ti_5O_{12} + 6Na^+ + 6e^- = Li_7Ti_5O_{12} + Na_6LiTi_5O_{12} \quad (1)$$

The LTO as an anode in NICs has a lower working potential plateau for the Na-ion intercalation reaction (0.9 V vs Na, which is equivalent to 1.2 V vs Li) than for the Li^+ ion intercalation reaction (1.55 V vs Li). Therefore, shifting the LTO to the Na^+ ion system from the Li^+ ion system increases the cell voltage, resulting in enhanced energy density for NICs compared to LICs. Density functional theory (DFT) simulations, in situ synchrotron X-ray diffraction, and advanced scanning transmission electron microscope imaging techniques are used to investigate the Na-insertion/extraction process of LTO. The NICs constructed with

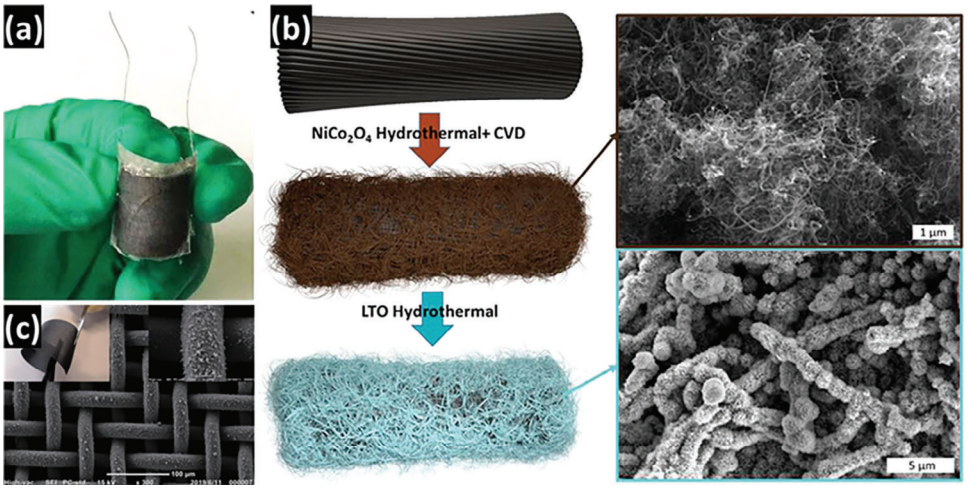

Figure 5. (a) Optical image of HSC. Reprinted with ref. [66] Copyright 2015, The Authors under a Creative Commons Attribution 4.0 International License, Published by Springer-Nature, (b) scheme showing the synthetic steps of the hybrid fiber electrode. Reprinted with permission.[67] Copyright 2019, Elsevier, and (c) SEM microphotographs of LTO/N-C@SSM. Reprinted with permission.[68]. Copyright 2020, The Chemical Society of Japan.

rGO sheets decorated with ≈50 nm LTO nanoparticles as the anode and AC as the cathode delivered a high energy density of 83 Wh kg^{-1} (with excellent capacity retention of 93% after 30 000 cycles), which was twice as high as that of the AC/(LTO-rGO)-based LICs (42 Wh kg^{-1}).[20] Schematic representations of the voltage profiles of the LTO anode and AC cathode in AC/LTO NHCs and LHCs and their corresponding energy/power densities are displayed in **Figures 4**a,b. To broaden the potential window, another attempt was made using mixed sodium and lithium solvents as electrolytes, which effectively enhanced the energy density without sacrificing power density and provided new insights into large-scale energy storage. In such a hybrid electrolyte system, the potential of Li and Na intercalation is different during the charging and discharging process; as a result, Li^+ and Na^+ intercalation can be carried out simultaneously. The lithium–sodium hybrid-ion capacitor (L/NIC) fabricated with LTO microspheres (LTO MS) as the anode and peanut shell-derived carbon as the cathode, and a mixed Na/Li electrolyte displayed the highest gravimetric energy density (≈65.3 Wh kg^{-1}) with remarkable cycling stability of 95% after 3000 cycles.[65] Figure 4c represents the CV curves of the NIC, LIC, and L/NIC hybrid capacitors at a scan rate of 5 mV s^{-1}. The Ragone plots and the cycling performance over 3000 cycles for all three are presented in Figures 4d,e.

5. Flexible LICs

In addition, flexible LICs are considered the "LICs for the future." Flexible LICs can maintain their characteristic shape even after being bent or twisted. Flexible LICs, in turn, can be applied to wearable devices. There are few reports on wearable LIBs/LICs, and research on this topic is in progress. Zuo et al.[66] reported a flexible LIC with excellent energy and power characteristics using LTO/carbon cloth for the first time. These researchers constructed a thin-film HSC with binder-free electrodes where the active material is directly grown on a highly porous and conductive carbon cloth (**Figure 5**a). The multiwalled carbon nanotube cathode and LTO nanowire array anode full-cell exhibited a high volumetric energy density and power density of ≈4.38×10^{-3} Wh L^{-1} and ≈0.565 kW L^{-1}, respectively, with excellent cycling stability over 3000 cycles. Dong et al.[22] fabricated an LIC with an LTO anode and an N-doped carbon nanotube (CNT) cathode without the use of any conductive carbon, binder, or current collector. They coated the LTO nanoplate arrays on a carbon textile by a simple one-pot hydrothermal reaction. The fabricated device delivered a maximum energy density of 76 Wh kg^{-1} and a power density of 0.567 kW kg^{-1}. Moreover, the LIC delivered long-term cyclic stability of 79% after 5000 charge–discharge cycles. In another study, N-doped CNT was used as the current collector for an LIC with an LTO anode and a hybrid N-doped CNT as the cathode.[67] The LIC delivered an energy density of 68 Wh kg^{-1} and a power density of 0.126 kW kg^{-1} (Figure 5b). Similar work on flexible electrodes was reported by Zhou et al.[68] where the obtained energy and power density of a LIC with an LTO/N-doped carbon@stainless steel mesh (LTO/N-C@SSM) anode and an AC cathode were 125 Wh kg^{-1} and 3.5 kW kg^{-1}, respectively (Figure 5c).

6. Summary and Outlook

Although LTO has been proposed as a better alternative to carbon-based negative electrodes, its commercial large-scale application in LICs is extremely limited. Purixel, developed by Pureechem, is an example of the commercialization of AC/LTO-based LICs.[69] LTO nanocrystals can be used as the anode to improve the stability and charging speed of existing LIBs and EDLCs. However, poor electronic conductivity, restricted alkali metal-ion diffusion, high manufacturing costs (the cost per kWh is comparatively high because of the low energy density of the cells), and unexpected gas evolution (especially at elevated temperatures) are the main challenges. The following methods could tackle these to a certain extent before LTO-based LICs are produced for the market:

1) An optimum pre-lithiation step can help avoid a sudden drop/rise during the initial charge/discharge and effectively

reduce capacity fading, ensuring improved cycling stability of the LIC assembly.

2) Balancing the anode-to-cathode mass ratio or volume ratio helps lower the diffusion resistance and drastically increases the rate performance. Various synthetic methods can be adopted to tune the structure of LTO to a more crystalline and nanoscale regime, which results in an enhanced Li^+ ion diffusion coefficient and electrical conductivity.
3) An optimum level of carbon coating and incorporation of conductive additives into the layers of the LTO material help to enhance the rate capability and cycling stability and facilitate fast ion transport during the lithiation/de-lithiation process.
4) The decomposition of electrolytes results in swelling of the anode through gassing and is the main issue to be addressed while tuning the electrolyte. Adding a supporting electrolyte or introducing a dual-ion concept to the Li-based electrolyte can reduce gassing and enhance ionic conductivity, translating to a LIC with a better performance.
5) Incorporation of the solvent-free coating process into electrode formulation will stimulate the development of present-day technologies, resulting in a large electrochemically active electrode surface area.

Even though the main contribution of energy density to the LIC is provided by the anode, the cathode also has a vital role in enhancing the diffusion rate and charge transfer, thereby increasing power density and long-term cyclic performance. Rather than using commercially available activated carbon, the derivation and activation of carbon from various natural sources have resulted in tremendous improvements in the performance of LICs. Different waste byproducts, as well as environmentally harmful materials, can be transformed into high-surface-area cathodes, combining the 2Rs: reuse and recycle. However, achieving the desired morphology for the AC derived from these materials is tricky. Hence, various polymer sources have been introduced as precursors of AC. High-surface-area and porous carbonaceous materials derived from natural sources improve LIC's overall performance and generate a boon out of waste. On the other hand, exploring the Na-ion chemistry for the LTO anode is complicated, and NICs are in their infancy. Further in-depth studies are thus required to bring NICs into a commercial reality.

Acknowledgements

M.A. and S.J. contributed equally to this work. SJ thank the Prime Minister's Research Fellowship (0902009) for financial support. YSL acknowledges the financial support from the National Research Foundation of Korea (NRF) through a grant funded by the Korean government (Ministry of Science, ICT, and Future Planning) (No. RS-2023-00208361). VA acknowledges financial support from the Science and Engineering Research Board, a statutory body of the Department of Science and Technology, Government of India, through the Swarnajayanti Fellowship (SB/SJF/2020-21/12).

Conflict of Interest

The authors declare no conflict of interest.

Keywords

activated carbon, energy density, $Li_4Ti_5O_{12}$ anode, Li-ion capacitors, Na-ion capacitors

Received: August 21, 2023
Revised: November 7, 2023
Published online:

[1] C. W. Babbitt, *Clean Technol. Environ. Policy* **2020**, *22*, 1213.
[2] J. B. Goodenough, *Acc. Chem. Res.* **2013**, *46*, 1053.
[3] M. Li, J. Lu, Z. Chen, K. Amine, *Adv. Mater.* **2018**, *30*, 1800561.
[4] L. Dong, W. Yang, W. Yang, Y. Li, W. Wu, G. Wang, *J. Mater. Chem. A* **2019**, *7*, 13810.
[5] J. Ding, W. Hu, E. Paek, D. Mitlin, *Chem. Rev.* **2018**, *118*, 6457.
[6] A. Jagadale, X. Zhou, R. Xiong, D. P. Dubal, J. Xu, S. Yang, *Energy Storage Mater.* **2019**, *19*, 314.
[7] J. J. Lamb, O. S. Burheim, *Energies* **2021**, *14*, 979.
[8] J. Liang, D.-W. Wang, *Adv. Energy Mater.* **2022**, *12*, 2200920.
[9] A. Muzaffar, M. B. Ahamed, K. Deshmukh, J. Thirumalai, *Renew. Sustain. Energy Rev.* **2019**, *101*, 123.
[10] L. Caizán-Juanarena, M. Arnaiz, E. Gucciardi, L. Oca, E. Bekaert, I. Gandiaga, J. Ajuria, *Adv. Energy Mater.* **2021**, *11*, 2100912.
[11] K. Naoi, S. Ishimoto, J.-I. Miyamoto, W. Naoi, *Energy Environ. Sci.* **2012**, *5*, 9363.
[12] G. G. Amatucci, F. Badway, A. Du Pasquier, T. Zheng, *J. Electrochem. Soc.* **2001**, *148*, A930.
[13] N. Xu, X. Sun, F. Zhao, X. Jin, X. Zhang, K. Wang, K. Huang, Y. Ma, *Electrochim. Acta* **2017**, *236*, 443.
[14] M. L. Divya, H.-Y. Lü, Y.-S. Lee, V. Aravindan, *Sustain. Energy Fuels* **2022**, *6*, 4884.
[15] K. Fleurbaey, N. Omar, J. Ronsmans, P. V. D. Bossche, J. V. Mierlo, presented at *5th European Symp. on SuperCapacitors and Hybrid Solutions*, Brasov, Romania, Apr **2007**.
[16] S. Dsoke, B. Fuchs, E. Gucciardi, M. Wohlfahrt-Mehrens, *J. Power Sources* **2015**, *282*, 385.
[17] J.-K. Lee, B.-G. Lee, J.-R. Yoon, *J. Nanosci. Nanotechnol.* **2015**, *15*, 8820.
[18] C. Lv, W. He, J. Jiang, E. Zhen, H. Dou, X. Zhang, *J. Power Sources* **2023**, *556*, 232487.
[19] S. Bhowmik, U. Bhattacharjee, S. Ghosh, S. K. Martha, *J. Energy Storage* **2023**, *73*, 109099.
[20] M.-S. Kim, H.-K. Roh, J. H. Jeong, G.-W. Lee, M. Nazarian-Samani, K. Y. Chung, K.-B. Kim, *J. Power Sources* **2019**, *409*, 48.
[21] K. Naoi, *Fuel Cells* **2010**, *10*, 825.
[22] S. Dong, H. Li, J. Wang, X. Zhang, X. Ji, *Nano Res.* **2017**, *10*, 4448.
[23] K. Leng, F. Zhang, L. Zhang, T. Zhang, Y. Wu, Y. Lu, Y. Huang, Y. Chen, *Nano Res.* **2013**, *6*, 581.
[24] N. Xu, X. Sun, X. Zhang, K. Wang, Y. Ma, *RSC Adv.* **2015**, *5*, 94361.
[25] X. Zhang, C. Lu, H. Peng, X. Wang, Y. Zhang, Z. Wang, Y. Zhong, G. Wang, *Electrochim. Acta* **2017**, *246*, 1237.
[26] K. Naoi, W. Naoi, S. Aoyagi, J.-I. Miyamoto, T. Kamino, *Acc. Chem. Res.* **2013**, *46*, 1075.
[27] K. Naoi, S. Ishimoto, Y. Isobe, S. Aoyagi, *J. Power Sources* **2010**, *195*, 6250.
[28] G. Wang, C. Lu, X. Zhang, B. Wan, H. Liu, M. Xia, H. Gou, G. Xin, J. Lian, Y. Zhang, *Nano Energy* **2017**, *36*, 46.
[29] I. Batsukh, S. Lkhagvajav, M. Adiya, S. Galsan, M. Bat-Erdene, P. Myagmarsereejid, *Ceram. Int.* **2023**, *49*, 26313.
[30] H. Raj, S. Saxena, A. Sil, *Mater. Today Proc.* **2019**, *18*, 2625.
[31] L. Cheng, H.-J. Liu, J.-J. Zhang, H.-M. Xiong, Y.-Y. Xia, *J. Electrochem. Soc.* **2006**, *153*, 1472.
[32] K. Hata, D. N. Futaba, K. Mizuno, T. Namai, M. Yumura, S. Iijima, *Science (80-.).* **2004**, *306*, 1362.
[33] B.-G. Lee, H.-J. Ahn, J.-R. Yoon, *Curr. Appl. Phys.* **2017**, *17*, 121.
[34] C. Jiang, J. Zhao, H. Wu, Z. Zou, R. Huang, *J. Power Sources* **2018**, *401*, 135.

[35] D. Ruan, M.-S. Kim, B. Yang, J. Qin, K.-B. Kim, S.-H. Lee, Q. Liu, L. Tan, Z. Qiao, *J. Power Sources* **2017**, *366*, 200.
[36] A. Jain, V. Aravindan, S. Jayaraman, P. S. Kumar, R. Balasubramanian, S. Ramakrishna, S. Madhavi, M. P. Srinivasan, *Sci. Rep.* **2013**, *3*, 3002.
[37] D. Puthusseri, V. Aravindan, B. Anothumakkool, S. Kurungot, S. Madhavi, S. Ogale, *Small* **2014**, *10*, 4395.
[38] D. Kalpana, S. H. Cho, S. B. Lee, Y. S. Lee, R. Misra, N. G. Renganathan, *J. Power Sources* **2009**, *190*, 587.
[39] R. Satish, A. Vanchiappan, C. L. Wong, K. W. Ng, M. Srinivasan, *Electrochim. Acta* **2015**, *182*, 474.
[40] P. Sennu, H.-J. Choi, S.-G. Baek, V. Aravindan, Y.-S. Lee, *Carbon N. Y.* **2016**, *98*, 58.
[41] B. Babu, P. G. Lashmi, M. M. Shaijumon, *Electrochim. Acta* **2016**, *211*, 289.
[42] A. Jain, S. Jayaraman, M. Ulaganathan, R. Balasubramanian, V. Aravindan, M. P. Srinivasan, S. Madhavi, *Electrochim. Acta* **2017**, *228*, 131.
[43] M. Maharjan, M. Ulaganathan, V. Aravindan, S. Sreejith, Q. Yan, S. Madhavi, J.-Y. Wang, T. M. Lim, *ChemistrySelect* **2017**, *2*, 5051.
[44] B. Li, H. Zhang, D. Wang, H. Lv, C. Zhang, *RSC Adv.* **2017**, *7*, 37923.
[45] Y.-T. Lin, C.-W. Chang-Jian, T.-H. Hsieh, J.-H. Huang, H. Chu Weng, Y.-S. Hsiao, W.-L. Syu, C.-P. Chen, *Appl. Surf. Sci.* **2021**, *543*, 148717.
[46] A. G. Elang Barruna, R. Muhamad Naufal, M. R. Nugraha, I. Subiyanto, N. Tinaprilla, A. Subhan, H. Chairul, *IOP Conf. Ser. Earth Environ. Sci.* **2021**, *673*, 012018.
[47] D. Puthusseri, V. Aravindan, S. Madhavi, S. Ogale, *Electrochim. Acta* **2014**, *130*, 766.
[48] R. Gokhale, V. Aravindan, P. Yadav, S. Jain, D. Phase, S. Madhavi, S. Ogale, *Carbon N. Y.* **2014**, *80*, 462.
[49] S. Chhatre, V. Aravindan, D. Puthusseri, A. Banerjee, S. Madhavi, P. P. Wadgaonkar, S. Ogale, *Mater. Today Commun.* **2015**, *4*, 166.
[50] H. Gao, D. Zhang, H. Zhou, J. Wu, C. Liu, G. Xu, M. Liu, J. Yang, *Vacuum* **2020**, *177*, 109360.
[51] V. Aravindan, D. Mhamane, W. C. Ling, S. Ogale, S. Madhavi, *ChemSusChem* **2013**, *6*, 2240.
[52] A. Banerjee, K. K. Upadhyay, D. Puthusseri, V. Aravindan, S. Madhavi, S. Ogale, *Nanoscale* **2014**, *6*, 4387.
[53] L. Ye, Q. Liang, Y. Lei, X. Yu, C. Han, W. Shen, Z.-H. Huang, F. Kang, Q.-H. Yang, *J. Power Sources* **2015**, *282*, 174.
[54] D. Mhamane, V. Aravindan, M.-S. Kim, H.-K. Kim, K. C. Roh, D. Ruan, S. H. Lee, M. Srinivasan, K.-B. Kim, *J. Mater. Chem. A* **2016**, *4*, 5578.
[55] X. Ma, L. Zhao, X. Song, Z. Yu, L. Zhao, Y. Yu, Z. Xiao, G. Ning, J. Gao, *Carbon N. Y.* **2018**, *140*, 314.
[56] A. Suryawanshi, M. Biswal, D. Mhamane, P. Yadav, A. Banerjee, P. Yadav, S. Patil, V. Aravindan, S. Madhavi, S. Ogale, *Appl. Mater. Today* **2016**, *2*, 1.
[57] Y. Chikaoka, E. Iwama, S. Seto, Y. Okuno, T. Shirane, T. Ueda, W. Naoi, M. T. H. Reid, K. Naoi, *Electrochim. Acta* **2021**, *368*, 137619.
[58] Y. Chikaoka, E. Iwama, T. Ueda, N. Miyashita, S. Seto, M. Sakurai, W. Naoi, M. T. H. Reid, P. Simon, K. Naoi, *J. Phys. Chem. C* **2020**, *124*, 12230.
[59] E. Iwama, T. Ueda, Y. Ishihara, K. Ohshima, W. Naoi, M. T. H. Reid, K. Naoi, *Electrochim. Acta* **2019**, *301*, 312.
[60] Y. Chikaoka, E. Iwama, M. Sakurai, T. Ueda, T. Shirane, W. Naoi, K. Naoi, *J. Phys. Chem. C* **2021**, *125*, 5995.
[61] Y. Chikaoka, R. Ochi, K. Fujii, T. Ariga, M. Sakurai, A. Matsumoto, T. Ueda, E. Iwama, K. Naoi, *J. Phys. Chem. C* **2022**, *126*, 14389.
[62] P. P. M. Schleker, C. Grosu, M. Paulus, P. Jakes, R. Schlögl, R.-A. Eichel, C. Scheurer, J. Granwehr, *Commun. Chem.* **2023**, *6*, 113.
[63] Z. An, X. Xu, L. Fan, C. Yang, *Electronics.* **2021**, *10*, 2623.
[64] S. Natarajan, K. Subramanyan, V. Aravindan, *Small* **2019**, *15*, 1904484.
[65] Z. Chen, Z. Li, W. He, Y. An, L. Shen, H. Dou, X. Zhang, *J. Electroanal. Chem.* **2021**, *888*, 115202.
[66] W. Zuo, C. Wang, Y. Li, J. Liu, *Sci. Rep.* **2015**, *5*, 7780.
[67] S. N. Kanakaraj, Y.-Y. Hsieh, P. K. Adusei, B. Homan, Y. Fang, G. Zhang, S. Mishra, S. Gbordzoe, V. Shanov, *Carbon N. Y.* **2019**, *149*, 407.
[68] S. Zhou, N. Huang, J. Yan, H. Zhang, X. Li, *Chem. Lett.* **2020**, *49*, 337.
[69] http://eng.pureechem.com/index.php/home/menu/25 (accessed: November 2023).

